Converting $SrI_2:Eu^{2+}$ into a near infrared scintillator by Sm^{2+} co-doping

Awater, R. H.P.; Alekhin, M. S.; Biner, D. A.; Krämer, K. W.; Dorenbos, P.

DOI
10.1016/j.jlumin.2019.04.002

Publication date
2019

Document Version
Accepted author manuscript

Published in
Journal of Luminescence

Accepted Manuscript

Converting SrI_2:Eu^{2+} into a near infrared scintillator by Sm^{2+} co-doping

R.H.P. Awater, M.S. Alekhin, D.A. Biner, K.W. Krämer, P. Dorenbos

PII: S0022-2313(19)30299-6

DOI: https://doi.org/10.1016/j.jlumin.2019.04.002

Reference: LUMIN 16397

To appear in: *Journal of Luminescence*

Received Date: 21 February 2019

Revised Date: 2 April 2019

Accepted Date: 3 April 2019

Please cite this article as: R.H.P. Awater, M.S. Alekhin, D.A. Biner, K.W. Krämer, P. Dorenbos, Converting SrI_2:Eu^{2+} into a near infrared scintillator by Sm^{2+} co-doping, *Journal of Luminescence* (2019), doi: https://doi.org/10.1016/j.jlumin.2019.04.002.

Converting SrI_2:Eu^{2+} into a near infrared scintillator by Sm^{2+} co-doping

R.H.P. Awater[1], M.S. Alekhin[1], D.A. Biner[2], K.W. Krämer[2], P. Dorenbos[1,*]

[1] *Delft University of Technology,*

Faculty of Applied Sciences,

Department of Radiation Science and Technology,

Section Luminescence Materials,

Mekelweg 15, 2629 JB Delft, Netherlands

[2] *Department of Chemistry and Biochemistry,*

University of Bern, Freiestrasse 3,

CH-3012 Bern, Switzerland

[*] *corresponding author email:p.dorenbos@tudelft.nl*

(Dated: April 3, 2019)

Abstract

The luminescence and scintillation properties of SrI_2 single crystals doped with 5% Eu^{2+} and 0.05%, 0.2% and 0.5% Sm^{2+} are evaluated. X-ray excited and photoluminescence measurements show energy transfer from excited Eu^{2+} ions to Sm^{2+} ions. At a concentration of 0.5% Sm^{2+}, the luminescence consists almost entirely of 740 nm emission from Sm^{2+} 5d-4f transitions. Co-doping SrI_2:5% Eu^{2+} with Sm^{2+} provides a novel method to bypass the self-absorption problem encountered in large SrI_2:Eu^{2+} crystals and, at the same time, provides a unique near-infrared emitting scintillator with a light yield of approximately 40,000 photons/MeV.

I. INTRODUCTION

SrI_2:Eu^{2+} is a very good scintillator material with light yield claims up to 120,000 photons/MeV, good energy resolution of 2.8% for 662 keV gamma ray detection and a decay time of 1.2 μs [1, 2]. However, the scintillation properties of SrI_2:Eu^{2+} are greatly dependent on the temperature, Eu^{2+} concentration and crystal size. Increasing the Eu^{2+} concentration, the crystal size or temperature results in an increased decay time and poorer scintillation performance [3, 4].

Photons emitted by Eu^{2+} can be re-absorbed by another Eu^{2+} ion, a process known as self-absorption. The absorption of the scintillation light can occur multiple times, delaying the scintillation light to exit the crystal and thus increasing the scintillation decay time. Since the quantum efficiency of Eu emission is not 100%, energy is lost non-radiatively and consequently the scintillation light yield decreases with each re-absorption process. Therefore, the losses in light yield due to self-absorption are most pronounced for larger crystals and for high concentrations of Eu^{2+} [5, 6]. In applying SrI_2:Eu^{2+} scintillator crystals in commercial sized detector systems, self-absorption is a major issue degrading the excellent scintillation properties found in small SrI_2:5% Eu^{2+} crystal samples. To compensate for the poorer performance of larger crystals, the Eu^{2+} concentration can be decreased [7]. By using digital readout electronics, purification of the feedstock, or by using tapered crystal shapes, the effects of self-absorption can be reduced. A review on those attempts can be found in [8]. Despite those improvements the self-absorption remains an issue of concern in case of larger than 1"$\times$1" crysyal sizes.

Recently, Alekhin *et al.* showed that the scintillation properties of SrI_2:Sm^{2+} are far less affected by self-absorption [9]. Interestingly, the broad 4f-5d excitations of Sm^{2+} (250 - 720 nm) spectrally overlap with the Eu^{2+} emission (420 - 450 nm). In this report, the energy transfer from Eu^{2+} to Sm^{2+} is investigated in samples of SrI_2 doped with both Eu^{2+} and Sm^{2+}. Ideally, all the deposited energy from the incoming radiation is transferred from Eu^{2+} to Sm^{2+} and consecutively emitted at Sm^{2+}, thereby limiting the self-absorption losses.

II. EXPERIMENTAL

The SrI_2:Eu^{2+},Sm^{2+} crystals were grown at the University of Bern by the vertical Bridgman technique in sealed quartz ampoules and contained a nominal dopant concentration of 5% Eu^{2+} and 0%, 0.05%, 0.2% or 0.5% Sm^{2+}. The crystals were grown as ingots of which the studied samples were cleaved. A photograph of the 0% and 0.05%, 0.2% and 0.5% Sm^{2+} doped SrI_2:5% Eu^{2+} samples is shown in Figure 1. Due to the hygroscopic nature of SrI_2 crystals, all samples were handled in a N_2 filled M-Braun UNILAB glovebox with a moisture content less than 1 ppm or mounted on a sealed Janis VPF-800 cryostat. The cryostat used in this study was baked out to remove all water before mounting the crystal samples and was used in combination with a Lakeshore 331 temperature controller for temperature dependent measurements.

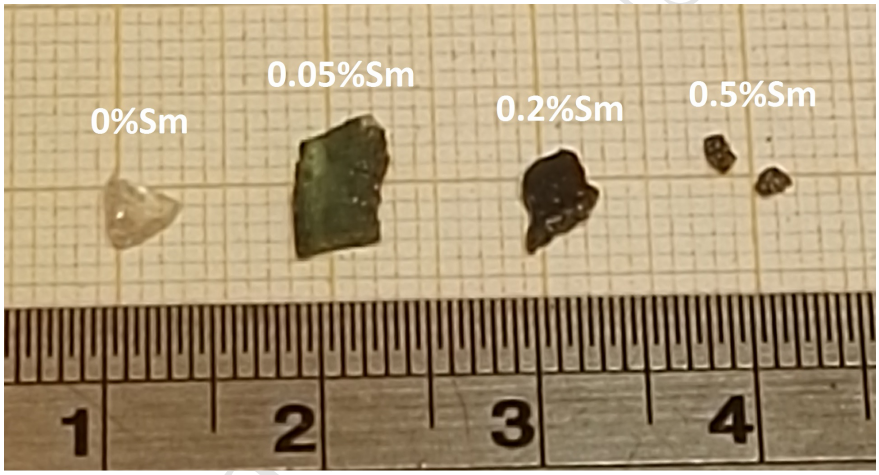

FIG. 1: Picture of the SrI_2:5% Eu^{2+} crystals with (from left to right) 0%, 0.05%, 0.2% and 0.5% Sm^{2+} doping concentration.

Scintillation pulse height spectra were recorded inside the N_2-filled glovebox using a ^{137}Cs 662 keV gamma source. A window-less Advanced Photonix APD (type 630-70-72-510) was used as photon detector, which was operated at 1600 V and cooled to 250 K. The output signal was amplified and shaped with a shaping time of 6 μs by an ORTEC 672 spectroscopic amplifier. To maximize the light collection, the scintillator samples were packed in Teflon using the pressed powder method described in Ref. [10]. By comparing the position of the 662 keV scintillation peak with the position of the 17.8 keV X-rays of an ^{241}Am source detected directly in the APD, the absolute electron-hole pair yield Y_{pe} can be obtained.

Assuming 100% quantum efficiency of the APD according to Ref. [11], only a correction for the reflectivity of the Teflon is required and thus the absolute light yield Y_{ph} is obtained using Y_{ph}=Y_{pe}/0.98.

X-ray excited luminescence (XEL) spectra were recorded using an X-ray tube with Cu anode operating at 60 kV and 25 mA. The emission of the samples was focused via a quartz window and a lens on the entrance slit of an ARC VM504 monochromator, dispersed, and recorded with a Hamamatsu R94302 PMT. The spectra were corrected for the monochromator transmission and the quantum efficiency of the PMT.

Photoluminescence (PL) excitation and emission spectra were recorded using a Newport 66921 Xe lamp in combination with a Horiba Gemini - 180 double grating monochromator. The emission light of the crystal was detected by a Hamamatsu C9100-13 EM-CCD camera. The excitation spectra were corrected for the lamp spectrum while no further correction was applied for the emission spectra. Appropriate cut-off filters were used to block second order transmission of the monochromators.

The time correlated single photon counting method using a pulsed picosecond X-ray source was used to record the scintillation decay time profiles. The X-ray tube was operated at a voltage of 40 kV. A HP 8116A Pulse/Function generator in combination with a Picoquant Sepia multi-channel laser diode were used to trigger the X-ray pulses. An IDQ id100 single photon detection module was used to detect the scintillation light.

III. RESULTS

The X-ray excited luminescence spectra of the studied SrI_2:Eu^{2+},Sm^{2+} crystals are shown in Figure 2. The spectra are normalized to the same integrated intensity. The emission band observed at 430 nm originates from the Eu^{2+} $4f^6 5d \rightarrow 4f^7$ transition. The 750 nm emission band is due to the Sm^{2+} $4f^5 5d \rightarrow 4f^6[^7F_0]$ transition. The $4f^5 5d \rightarrow 4f^6[^7F_{1-6}]$ transitions will contribute to the long wavelength side of the emission band [9]. Due to poor optical quality and the small size of the 0.5% Sm^{2+} sample, the emission spectrum is considerably more noisy.

Figure 3 shows part of the ^{137}Cs pulse-height spectra of the SrI_2:Eu^{2+},Sm^{2+} crystals measured with an avalanche photodiode. The 662 keV full absorption peaks appear between channels 440 to 600 and the Compton edges are seen between channels 300 and 450. The

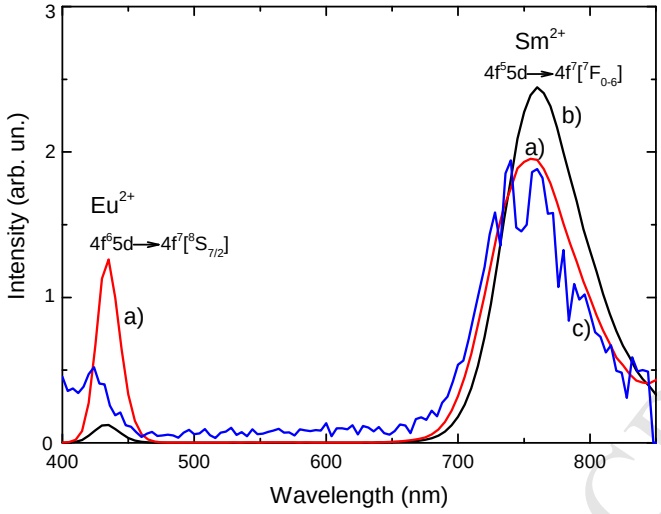

FIG. 2: Normalized X-ray excited luminescence spectra of SrI_2:5% Eu^{2+} with a) 0.05%, b) 0.2% and c) 0.5% Sm^{2+} measured at room temperature.

light yield and energy resolution of the crystals are derived from the 662 keV full absorption peak and are summarized in Table I. Due to the small crystal dimensions, an iodide X-ray escape peak is observed at approximately 30 keV lower energy than the full absorption peak for the sample without Sm^{2+}. As a result of the poor energy resolution of the samples containing Sm^{2+}, the escape peak is observed as a shoulder band.

TABLE I: Light yield (LY) and energy resolution (R) of SrI_2:5% Eu^{2+} with different concentrations of Sm^{2+} as derived from pulse height measurements recorded under 662 keV γ-ray excitation at 250 K with an avalanche photodiode.

Sample	[Sm^{2+}] (%)	LY (ph/MeV)	R (%)
SrI_2:5% Eu^{2+}	0	40500	3.8
	0.05	39500	7.6
	0.2	33000	7.8
	0.5	42000	10.5

Figure 4 shows the photoluminescence excitation and emission spectra of the SrI_2:Eu^{2+},Sm^{2+} samples measured at room temperature. The excitation spectra were recorded by monitoring the 740 nm Sm^{2+} 5d-4f emission. The emission spectra were recorded

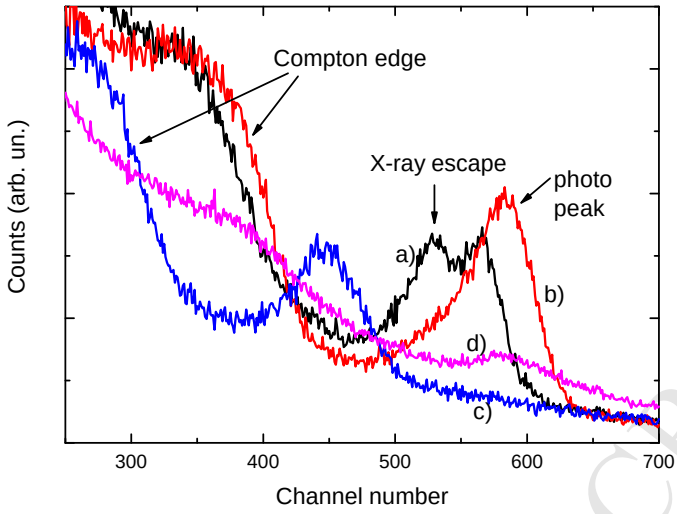

FIG. 3: Pulse-height spectra of a ^{137}Cs source measured with the SrI_2:5% Eu^{2+} samples doped with a) 0%, b) 0.05%, c) 0.2% and d) 0.5% Sm^{2+} at 250 K with an avalanche photodiode. Only the part around the Compton edge and 662 keV total absorptin peak is shown.

under 370 nm excitation where 4f-5d excitation of both Eu^{2+} and Sm^{2+} occurs.

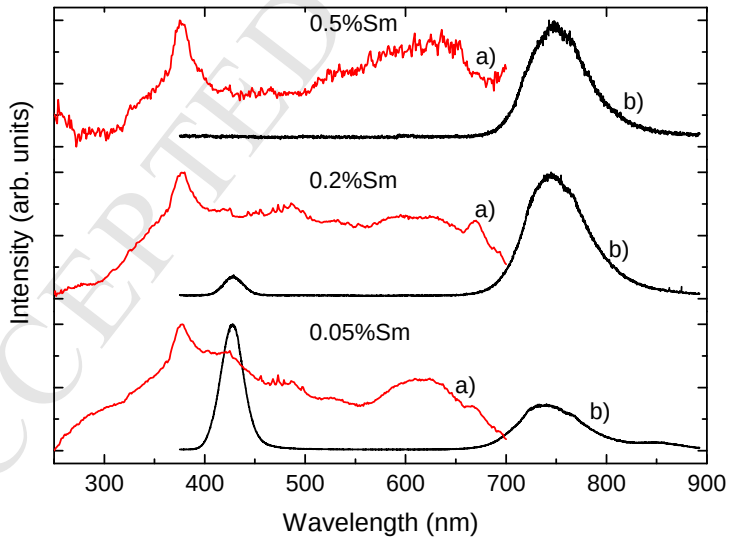

FIG. 4: Photoluminescence excitation spectra a) of 740 nm emission, and b) emission spectra at 370 nm excitation of SrI_2:5% Eu^{2+} with 0.5%, 0.2% and 0.05% Sm^{2+} measured at room temperature.

Figure 5 shows the scintillation decay profiles of the studied SrI_2:Eu^{2+},Sm^{2+} samples. The

scintillation decay profiles are well fitted by a single exponential function and the obtained decay times are plotted as a function of temperature in Figure 6.

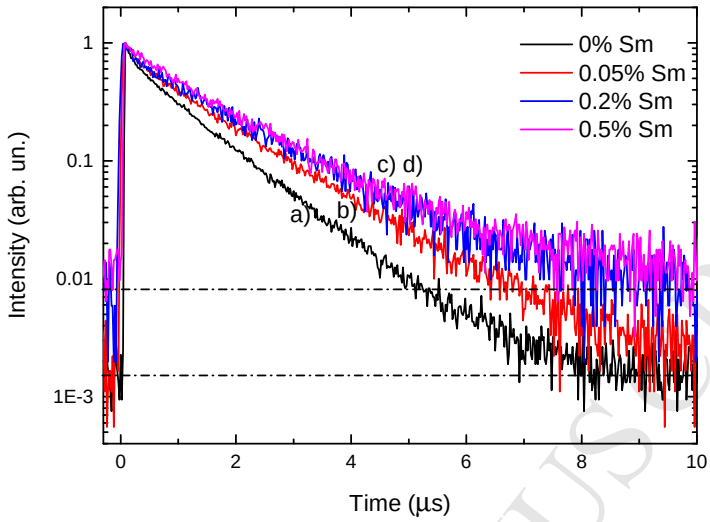

FIG. 5: Scintillation decay profiles of SrI_2:5% Eu^{2+} with a) 0%, b) 0.05%, c) 0.2% and d) 0.5% Sm^{2+} recorded at 300 K. The dashed horizontal lines indicate the background intensity for the crystals containing (top line) 0.2% Sm^{2+} and 0.5% Sm^{2+} and (bottom line) 0% Sm^{2+} and 0.05% Sm^{2+}.

IV. DISCUSSION

Curve a) in Figure 6 shows the temperature dependence of the scintillation decay time of SrI_2:5% Eu^{2+}, which increases from 0.6 μs to 1.7 μs when increasing the temperature from 100 K to 500 K. Increasing the temperature broadens the excitation and emission bands and consequently results in an increased spectral overlap between both bands. As described in Ref. [4], such increased overlap results in self-absorption of the emission light, which leads to longer scintillation decay and delayed emission. The scintillation decay time of the SrI_2:Eu^{2+},Sm^{2+} doped samples shown as curves b), c), and d) in Figure 6, increases linearly from approximately 1.2 μs to 1.7 μs when increasing the temperature from 100 K to 500 K. This is similar to the observed temperature dependence of the scintillation decay time in SrI_2:1% Sm^{2+} with the conclusion that Sm^{2+} emission is less affected by self-absorption [9].

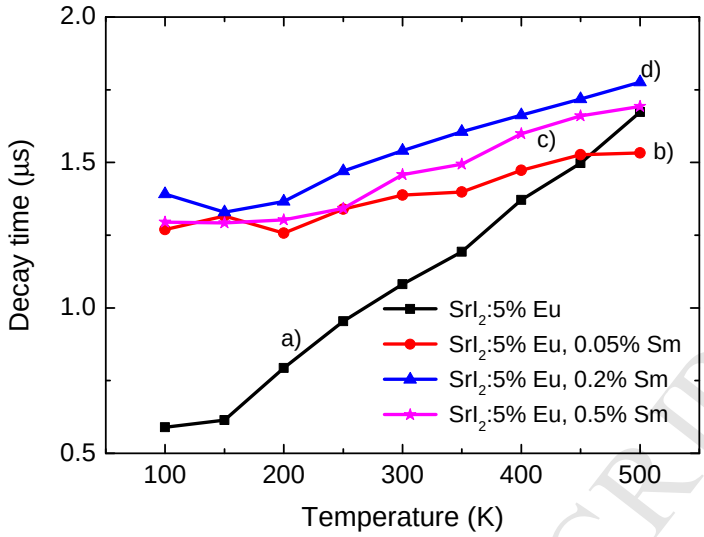

FIG. 6: Temperature dependence of the scintillation decay time constant of SrI_2:5% Eu^{2+} with a) 0%, b) 0.05%, c) 0.2% and d) 0.5% Sm^{2+}. The scintillation decay time constants are obtained by fitting the decay profiles with a single exponential component.

This appears also the case for the SrI_2:Eu^{2+},Sm^{2+} samples.

Figure 7 is derived from results in Ref. [9] and shows the vacuum referred binding energies of an electron in the 4f and 5d levels of Sm^{2+} and Eu^{2+} ions and in the host valence and conduction band. Initially, the deposited energy from the incoming radiation creates electron-hole pairs that migrate through the lattice and can be captured by a luminescence recombination center. This is illustrated by the dotted lines in Figure 7. In the case of SrI_2 doped with both Eu^{2+} and Sm^{2+}, the charge carriers can migrate to and recombine on either Eu^{2+} or Sm^{2+} ions. However, Eu^{2+} appears a far better luminescence recombination center than Sm^{2+}, hence the better scintillation properties of SrI_2:5 %Eu^{2+} (120,000 ph/MeV) compared to SrI_2:1% Sm^{2+} (6000 ph/MeV). Indeed both Eu^{2+} and Sm^{2+} emission are observed in the XEL spectra of the SrI_2:Eu^{2+},Sm^{2+} samples shown in Figure 2. Based on the pulse-height measurements in Figure 3 a comparable light-yield of approximately 40,000 ph/MeV for all four studied samples, as listed in Table I, is obtained. We therefore normalized the XEL spectra in Fig. 2 to the same integrated intensity. Figure 2 shows that the relative Eu^{2+} emission intensity decreases with Sm^{2+} concentration but for all concentrations its intensity is much less than that of Sm^{2+} emission. This implies either that at

0.05% Sm^{2+} co-doping the energy transfer from Eu to Sm is already very efficient, or that Sm^{2+} captures large part of the electrons and hole directly from the ionization track.

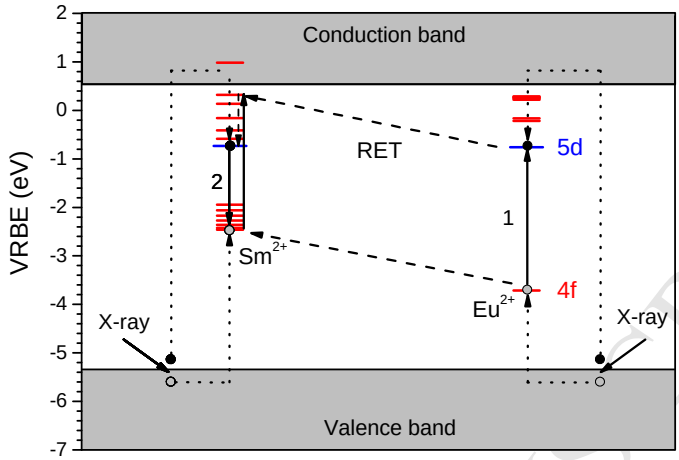

FIG. 7: Vacuum referred binding energy (VRBE) scheme for electrons in the 4f and 5d levels of Sm^{2+} and Eu^{2+} ions in a SrI_2 host lattice, illustrating the resonant energy transfer (RET) process from Eu^{2+} to Sm^{2+}. The arrows are explained in the text.

A similar observation is made for the photoluminescence (PL) emission measurements in Figure 4, *i.e.*, the Eu^{2+} emission decreases while the Sm^{2+} emission increases with increasing Sm^{2+} concentration. No Eu^{2+} emission is observed anymore for a concentration of 0.5% Sm^{2+}. The PL excitation spectra of the 740 nm Sm^{2+} emission shows both the Sm^{2+} and Eu^{2+} 4f-5d excitations between 300 and 675 nm and between 270 and 400 nm, respectively. The appearance of a peak near 380 nm is most likely an artefact because of a decreasing excitation efficiency at shorter wavelengths due to very strong Eu^{2+} absorption already near the sample surface.

The capture of the charge carriers by Eu^{2+}, brings the Eu^{2+} into the excited 5d state (arrow 1 in Figure 7). This excitation energy can then be transferred to a neighboring Sm^{2+} ion either via a radiative or non-radiative energy transfer process. In the case of radiative energy transfer, Sm^{2+} is excited after radiative decay of Eu^{2+}. This will lead to a rise time in the Sm^{2+} luminescence intensity curve of Figure 5 of the order of the radiative decay time of Eu^{2+}. Since such $\approx 1\mu$s long rise time is not observed, we conclude that a non-radiative

resonant energy transfer takes place. A higher concentration of Sm^{2+} results in a decrease in the average distance between an excited Eu^{2+} ion and a Sm^{2+} ion resulting in a higher rate of energy transfer. Therefore, increasing the Sm^{2+} concentration results in an increase of the Sm/Eu emission intensity ratio in the XEL and PL spectra while the total number of emitted photons remains the same. Once the energy is transferred to Sm^{2+} it is emitted as a photon (arrow 2). A value of 6000 ph/MeV was reported for SrI_2:1% Sm^{2+} [9]. For the SrI_2:5% Eu^{2+}, 0.5% Sm^{2+} sample a light yield of 42000 ph/MeV is observed. The X-ray excited and photoluminescence emission measurements showed that the emission consisted of almost exclusively Sm^{2+} emission. Therefore, Eu^{2+} transfers the absorbed energy efficiently to the Sm^{2+} luminescence centers.

The energy resolution of the ^{137}Cs 662 keV photo peak in Fig. 3 becomes worse when increasing the Sm^{2+} content, and for a concentration of 0.5% Sm^{2+} the photo peak is barely visible despite that all samples show comparable light yield of approximately 40,000 ph/MeV. The poor scintillation performance of the 0.5% Sm^{2+} sample is attributed to a poor optical quality of the sample. Note that those samples are also quite small, see Fig. 1.

V. CONCLUSIONS

The luminescence and scintillation properties of SrI_2 crystals doped with 5% Eu^{2+} and 0.05%, 0.2% or 0.5% Sm^{2+} were evaluated. X-ray excited luminescence and photoluminescence measurements showed both the 430 nm Eu^{2+} and the 740 nm Sm^{2+} 5d-4f emission bands. At a concentration 0.5% Sm^{2+}, the luminescence originated almost exclusively from Sm^{2+}. This was explained by a resonant energy transfer of the excited Eu^{2+} ions to the Sm^{2+} ions. The temperature dependence of the scintillation decay time indicates a significantly lower degree of self-absorption compared to standard SrI_2:5% Eu^{2+}. The 40,000 ph/MeV light yield and 740 nm Sm^{2+} emission make these crystals attractive for use in combination with photodiode detectors. Growing larger and better quality Sm^{2+} co-doped SrI_2:Eu^{2+} crystals is a viable method to bypass the self-absorption problem that limits the scintillation performance of standard SrI_2:5% Eu^{2+}.

Acknowledgments

This work was supported by the Dutch Technology Foundation STW, which is part of the Netherlands Organization for Scientific Research (NWO), and which is partly funded by the Ministry of Economic Affairs. This work was partly funded by Saint Gobain Crystals, France.

[1] C.M. Wilson, E.V. van Loef, J. Glodo, N. Cherepy, B. Hull, S. Payne, W.-S. Choong, W. Moses, K.S, Shah, Proc. Of SPIE 7079 (2008) 707917.

[2] N.J. Cherepy, G. Hull, A.D. Drobshoff, S.A. Payne, E. van Loef, C.M. Wilson, K.S. Shah, U.N. Roy, A. Burger, L.A. Boatner, W-S. Choong, W.W. Moses, Appl. Phys. Lett. 92 (2008) 083508.

[3] J. Glodo, E.V. van Loef, N. J. Cherepy, S.A. Payne, K.S. Shah, IEEE Trans. Nucl. Sci. 57 (2010) 1228.

[4] M.S. Alekhin, J.T.M. de Haas, K.W. Krämer, P. Dorenbos, IEEE Trans. Nucl. Sci.58 (2011) 2519.

[5] M.S. Alekhin, K.W. Krämer, P. Dorenbos, Nucl. Instr. Meth. A714 (2013) 13.

[6] L.A. Boatner, J.O. Ramey, J.A. Kolopus, R. Hawrami, W.M. Higgins, E. vanLoef, J. Glodo, K.S. Shah, Emmanuel Rowe, Pijush Bhattacharya, EugeneTupitsyn, Michael Groza, Arnold Burger, N.J. Cherepy d, S.A. Payne, Journal of Crystal Growth 379 (2013) 63.

[7] N.J. Cherepy, S.A. Payne, B.W. Sturm, *et al.*, IEEE Trans. Nucl. Sci. 60 (2013) 955.

[8] N. J. Cherepy, P. R. Beck, S. A. Payne, E. L. Swanberg, B. M. Wihl, S. E. Fisher, S. Hunter, P. A. Thelin, C. J. Delzer, S. Shahbazi, A. Burger, K. S. Shah, R. Hawrami, L. A. Boatner, M. Momayezi, K. Stevens, M. H. Randles, D. Solodovnikov, Hard X-ray, gamma-ray, and neutron detector physics XIX Book Series: Proceedings of SPIE 10392 (2017) Article Number1039202.

[9] M.S. Alekhin, R.H.P. Awater, Daniel A. Biner, K.W. Krämer, J. T.M. de Haas, P. Dorenbos, Journal of Luminescence 167 (2015) 347.

[10] J.T.M. de Haas, P. Dorenbos, IEEE Trans. Nucl. Sci. 55 (2008) 1086.

[11] J.T.M. de Haas, P. Dorenbos, C.W.E. van Eijk, Nucl. Instr. and Meth. 537 (2005) 97.